A Complex Least Squares Enhanced Smart DFT Technique for Power System Frequency Estimation

Yili Xia, *Member, IEEE*, Yukun He, Kai Wang, Wenjiang Pei, Zoran Blazic, and Danilo P. Mandic, *Fellow, IEEE*

***Abstract*—A complex-valued least-squares (CLS) framework is proposed in order to enhance the accuracy of the smart discrete Fourier transform (SDFT) algorithms for power system frequency estimation in the presence of noise and harmonic pollution. It is first established that the underlying time-series relationship among the consecutive DFT fundamental components employed by the original SDFT algorithms does not hold when noises or unexpected higher order harmonics are present, resulting in suboptimal estimation performances. To eliminate these adverse effects on the frequency estimation, the degree of the relationship breakdown is next quantified via a model mismatch error vector. The CLS technique is then employed to minimize the mean-square model deviation when the SDFT voltage modelling is suboptimal. The proposed CLS-enhanced SDFT (CLS-SDFT) methods are shown to be more accurate than the original ones in heavily noisy and harmonic-distorted environments, typical scenarios in online frequency estimation. The benefits of the SDFT framework are verified by simulations for various power system conditions, as well as for real-world measurements.**

***Index Terms*—Complex-valued least squares (CLS), discrete Fourier transform (DFT), frequency estimation.**

I. Introduction

SYSTEM frequency is a key parameter in the control of generation-load imbalance in power grids; it can be used, for instance, to determine the harmonic contents of currents drawn by nonlinear loads. Accurate frequency estimation is essential, since maintaining the nominal frequency value is a prerequisite for the stability of the grid and normal operation of electrical devices. Considering the power system voltage waveform as a pure sinusoid, the time between two zero crossings is an indication of system frequency [3]. However, in reality, the measured voltages are only available in a noisy or distorted form, and a variety of architectures and algorithms has been developed to cater for these scenarios. These include phase-locked loops (PLLs) [4], [5]; notch filters [6]; least-squares (LS) techniques and their variants [3], [7], [8]; adaptive filtering [9]–[11]; Kalman filtering [12], [13]; Taylor series [14], [15]; and iterative approaches [16]–[18].

The discrete Fourier transform (DFT)-based frequency estimation algorithms have been used in many aspects of power system analysis. However, the well-known coherent sampling properties of the DFT guarantee accurate frequency estimation only when the sampling frequency is an integer multiple of the power frequency of interest. In practice, coherent sampling is not guaranteed due to either the finite duration of data segments or random frequency fluctuations, yielding leakage and picket fence effects. To mitigate these effects and to improve the resolution of DFT in electric power systems, window functions are utilized to reduce the leakage effects, while the errors caused by picket fence effects are reduced by interpolation algorithms [19]–[26]. However, the interpolation schemes usually require a large number of samples (1024 samples or more) for the DFT operation, and this computational burden limits their usefulness in practical applications. Apart from the improved windowing functions and interpolation schemes, various algorithms have also been proposed to improve the DFT performance in the context of asynchronous sampling. The methods in [27] and [28] present correction algorithms based on the instantaneous phase-angle errors, while the method in [29] adjusts the sampling frequency in order to create synchronous sampling conditions. Digital filters were also used to attenuate the oscillations within the phase-angle involution of the DFT components that were used [30], [31]. The work in [32] introduces a recursive relationship between two consecutive fundamental components of the DFT in order to extract the instantaneous phasor and system frequency; however, the implicit synchronous sampling assumption results in a suboptimal performance when the system frequency deviates from its nominal value. To solve this problem, accurate recursive relationships among consecutive DFT fundamental components have been proposed, leading to simple but precise formulas to calculate the system frequency in the presence of higher order harmonics and frequency deviations. The performance advantages of such smart DFT (SDFT) algorithms over the conventional recursive DFT and Prony methods have been addressed in [1] and [2].

In this paper, a complex-valued least squares (CLS) framework is proposed to enhance the accuracy of smart discrete Fourier transform (SDFT) algorithms [1], [2] for power system

Manuscript received October 05, 2014; revised January 01, 2015; accepted February 14, 2015. Date of publication April 14, 2015; date of current version March 22, 2017. This work was supported by the National Natural Science Foundation of China under Grants 61201173, 61271058, and 61401094; the Specialized Research Fund for the Doctoral Program of Higher Education of China under Grant 20110092110008; and the Natural Science Foundation of Jiangsu Province under Grants SBK201140040, BK2011060, and BK20140645. Paper no. TPWRD-01217-2014.

Y. Xia, K. Wang, and W. Pei are with the School of Information Science and Engineering, Southeast University, Nanjing 210096, China (e-mail: yili.xia06@gmail.com; kaiwang@seu.edu.cn; wjpei@seu.edu.cn).

Y. He is with the School of Electronic Science and Engineering, Southeast University, Nanjing 210096, China (e-mail: hyk_seu@163.com).

Z. Blazic is with the Elektroprenos BiH a.d., 78000 Banja Luka, Bosnia and Herzegovina (e-mail: zoran.blazic@elprenos.com).

D. P. Mandic is with the Department of Electrical and Electronic Engineering, Imperial College London, London SW7 2BT, U.K. (e-mail: d.mandic@imperial.ac.uk).

Color versions of one or more of the figures in this paper are available online at http://ieeexplore.ieee.org.

Digital Object Identifier 10.1109/TPWRD.2015.2418778

frequency measurements in the presence of noise and unexpected harmonic pollution. It is first illustrated that the fundamental time-series relationship among the consecutive DFT fundamental components employed by the original SDFT algorithms does not hold in the presence of noises or higher order harmonics. For rigor, we first analyze the degree of this relationship breakdown within a sliding window of SDFT. The complex least squares (CLS) is then used in conjunction with SDFT to minimize the degree of model mismatch and provide enhanced frequency estimation in noisy and harmonic-distorted environments. The benefits of the proposed CLS-SDFT algorithms are verified by simulations in various power system conditions, as well as for a real-world measurement.

II. Derivation of the Proposed Complex Least-Squares Enhanced Smart DFT (SDFT) Algorithms

A. Original Smart DFT (SDFT) Algorithm

The voltages of a power system in a noise-free and harmonics-free environment can be represented in a discrete time form as

$$v(k) = A\cos(\omega k \triangle \mathrm{T} + \phi) \tag{1}$$

where A is the voltage amplitude, ϕ is the initial phase angle, $\omega = 2\pi f_{\mathrm{o}}$, and f_{o} is the nominal system frequency. For the sampling rate $f_s = 1/\Delta\mathrm{T} = Nf_{\mathrm{o}}$, where N is the number of samples per voltage cycle, the voltage $v(k)$ can be expressed as

$$\begin{aligned} v(k) &= \frac{Ae^{\jmath(\omega k\triangle \mathrm{T}+\phi)} + Ae^{-\jmath(\omega k\triangle \mathrm{T}+\phi)}}{2} \\ &= \frac{Ve^{\jmath\omega k\triangle \mathrm{T}} + V^* e^{-\jmath\omega k\triangle \mathrm{T}}}{2} \end{aligned} \tag{2}$$

where $V = Ae^{\jmath\phi}$ is the voltage phasor. The fundamental frequency component within the DFT of $v(k)$ is then given by

$$\hat{v}_n = \frac{2}{N}\sum_{k=0}^{N-1} v(k+n)e^{-\jmath 2\pi k/N}. \tag{3}$$

When the system frequency deviation is taken into consideration by setting $\omega = 2\pi(f_{\mathrm{o}} + \Delta f)$, from (2) and (3), we obtain

$$\begin{aligned} \hat{v}_n &= \frac{1}{N}\sum_{k=0}^{N-1} \big(Ve^{\jmath(2\pi(f_{\mathrm{o}}+\Delta f))(k+n)/Nf_{\mathrm{o}}} \\ &\quad + V^* e^{-\jmath(2\pi(f_{\mathrm{o}}+\Delta f))(k+n)/Nf_{\mathrm{o}}}\big)e^{-\jmath 2\pi k/N} \\ &= \frac{V}{N}e^{\jmath 2\pi n(f_{\mathrm{o}}+\Delta f)/Nf_{\mathrm{o}}}\sum_{k=0}^{N-1} e^{\jmath 2\pi k\Delta f/Nf_{\mathrm{o}}} \\ &\quad + \frac{V^*}{N}e^{-\jmath 2\pi n(f_{\mathrm{o}}+\Delta f)/Nf_{\mathrm{o}}}\sum_{k=0}^{N-1} e^{-\jmath 2\pi k(2f_{\mathrm{o}}+\Delta f)/Nf_{\mathrm{o}}} \\ &= \frac{V}{N}e^{\jmath 2\pi n(f_{\mathrm{o}}+\Delta f)/Nf_{\mathrm{o}}}e^{\jmath\pi(N-1)\Delta f/Nf_{\mathrm{o}}}\frac{\sin(\frac{\pi\Delta f}{f_{\mathrm{o}}})}{\sin(\frac{\pi\Delta f}{Nf_{\mathrm{o}}})} \\ &\quad + \frac{V^*}{N}e^{-\jmath 2\pi n(f_{\mathrm{o}}+\Delta f)/Nf_{\mathrm{o}}}e^{-\jmath\pi(N-1)(2f_{\mathrm{o}}+\Delta f)/Nf_{\mathrm{o}}} \\ &\quad \times \frac{\sin(\frac{\pi(2f_{\mathrm{o}}+\Delta f)}{f_{\mathrm{o}}})}{\sin(\frac{\pi(2f_{\mathrm{o}}+\Delta f)}{Nf_{\mathrm{o}}})}. \end{aligned} \tag{4}$$

Upon denoting the first term of (4) by a_n and the second term by b_n, then $\hat{v}_n$ in (4) can be written as

$$\hat{v}_n = a_n + b_n. \tag{5}$$

For simplicity, we shall denote the exponential kernel in (4) as

$$r = e^{\jmath 2\pi(f_{\mathrm{o}}+\Delta f)/Nf_{\mathrm{o}}}. \tag{6}$$

Then, from (4) and (5), it follows that:

$$a_n = ra_{n-1}, \text{and } b_n = r^{-1}b_{n-1} \tag{7}$$

and, therefore, the three consecutive DFT fundamental components based on (4) can be expressed as

$$\begin{aligned} \hat{v}_n &= a_n + b_n = ra_{n-1} + r^{-1}b_{n-1} \\ \hat{v}_{n-1} &= a_{n-1} + b_{n-1} \\ \hat{v}_{n-2} &= a_{n-2} + b_{n-2} = r^{-1}a_{n-1} + rb_{n-1}. \end{aligned} \tag{8}$$

After some algebraic manipulations of (8), the following time-series relationship among three consecutive DFT fundamental components can be found:

$$w\hat{v}_{n-1} = \hat{v}_n + \hat{v}_{n-2} \tag{9}$$

where

$$w = r + r^{-1} = 2\cos\left(\frac{2\pi(f_{\mathrm{o}}+\Delta f)}{Nf_{\mathrm{o}}}\right) \tag{10}$$

which can be estimated by

$$w = \frac{\hat{v}_n + \hat{v}_{n-2}}{\hat{v}_{n-1}}. \tag{11}$$

Therefore, the estimate of the system frequency $\hat{f}$ by the SDFT algorithm is given by [1]

$$\hat{f} = f_{\mathrm{o}} + \Delta f = \frac{f_s}{2\pi}\cos^{-1}\left(\frac{\Re(w)}{2}\right) \tag{12}$$

where $\Re(\cdot)$ denotes the real part of a complex number.

B. SDFT in the Presence of Harmonics

In the presence of an mth-order harmonic, the system voltages assume the form

$$v(k) = A\cos(\omega k\triangle \mathrm{T} + \phi) + A_m\cos(m\omega k\triangle \mathrm{T} + \phi_m). \tag{13}$$

Upon taking into consideration frequency deviation from the nominal frequency, the fundamental frequency component within the DFT of $v(k)$ can now be obtained as

$$\begin{aligned} \hat{v}_n &= \frac{2}{N}\sum_{k=0}^{N-1} v(k+n)e^{-\jmath 2\pi k/N} \\ &= \frac{1}{N}\sum_{k=0}^{N-1} \big(Ve^{\jmath(2\pi(f_{\mathrm{o}}+\Delta f))(k+n)/Nf_{\mathrm{o}}} \\ &\quad + V^* e^{-\jmath(2\pi(f_{\mathrm{o}}+\Delta f))(k+n)/Nf_{\mathrm{o}}} \\ &\quad + V_m e^{\jmath(2\pi m(f_{\mathrm{o}}+\Delta f))(k+n)/Nf_{\mathrm{o}}} \\ &\quad + V_m^* e^{-\jmath(2\pi m(f_{\mathrm{o}}+\Delta f))(k+n)/Nf_{\mathrm{o}}}\big)e^{-\jmath 2\pi k/N} \end{aligned}$$

$$= a_n + b_n + \frac{V_m}{N} r^{mn} e^{\jmath\pi m(N-1)\Delta f/Nf_\circ} \frac{\sin(\frac{\pi m\Delta f}{f_\circ})}{\sin(\frac{\pi m\Delta f}{Nf_\circ})} + \frac{V_m^*}{N} r^{-mn} e^{-\jmath\pi m(N-1)(2f_\circ+\Delta f)/Nf_\circ} \frac{\sin(\frac{\pi m(2f_\circ+\Delta f)}{f_\circ})}{\sin(\frac{\pi m(2f_\circ+\Delta f)}{Nf_\circ})}. \quad (14)$$

We shall denote the third and the fourth terms by c_n and d_n, respectively, then (14) can be simplified as

$$\hat{v}_n = a_n + b_n + c_n + d_n \quad (15)$$

to give the following relationships within two consecutive DFT fundamental components:

$$\begin{aligned} a_n &= r a_{n-1}, \quad b_n = r^{-1} b_{n-1}, \\ c_n &= r^m c_{n-1}, \quad d_n = r^{-m} d_{n-1}. \end{aligned} \quad (16)$$

We can now construct a new variable $\hat{p}_n$ as

$$\begin{aligned} \hat{p}_n &= (r^m + r^{-m})\hat{v}_n - (\hat{v}_{n-2} + \hat{v}_n) \\ &= f(w)\hat{v}_n - (\hat{v}_{n-2} + \hat{v}_n) \end{aligned} \quad (17)$$

and use a general polynomial function $f(w)$ of $w = r + r^{-1}$ to represent $r^m + r^{-m}$ for any integer[1] m. Based on (17), the following time-series relationship among three consecutive samples of p_n holds

$$w\hat{p}_{n-1} = \hat{p}_n + \hat{p}_{n-2}. \quad (18)$$

Upon substituting (17) into (18), and after a few algebraic manipulations, we obtain the polynomial equation employed by the so-called SDFT$_m$ algorithm to estimate w, given by

$$wf(w)\hat{v}_{n-2} - (w + f(w))(\hat{v}_{n-3} + \hat{v}_{n-1}) + \hat{v}_{n-4} + 2\hat{v}_{n-2} + \hat{v}_n = 0. \quad (19)$$

Now that the variable w has been determined, the SDFT$_m$ algorithm gives the estimated system frequency using (12).

Remark 1: Although the principle behind the SDFT frequency estimation algorithms is theoretically correct, these algorithms are inaccurate when the voltage samples contain noise or unexpected higher order harmonics, since in such situations, the equalities in (9) and (18) do not hold and an implicit real-valued property of $w = r + r^{-1}$ is likely to be violated.

Although the original SDFT algorithms aim to use $\Re(w)$ in the argument of (12) to eliminate the effects of noise and higher order harmonics pollution on the performance of frequency estimation, this does not address the root of the problem—the incoherent sampling for DFT algorithms, which, in turn, renders frequency estimates $\hat{f}$ inaccurate.

[1]Note that using (6), we have $r^m + r^{-m} = 2\cos(mx)$, where for notation simplicity, we define $x = 2\pi(f_\circ + \Delta f)/Nf_\circ$. The term $\cos(mx)$ can be represented by $\cos(x)$ using the Chebyshev polynomials $T_m(\cdot)$ of the first kind as $\cos(mx) = T_m(\cos(x))$, and the unique polynomials can be defined by the recurrent relation as $T_0(\cos(x)) = 1$, $T_1(\cos(x)) = \cos(x)$, and $T_m(\cos(x)) = 2\cos(x)T_{m-1}(\cos(x)) - T_{m-2}(\cos(x))$. Therefore, $r^m + r^{-m}$ can be uniquely represented as a polynomial function $f(w)$ of w, where $w = r + r^{-1} = 2\cos(x)$.

C. Complex-Valued Least-Squares Enhanced Smart DFT (CLS-SDFT) Algorithms

To solve the aforementioned problems encountered by the original SDFT algorithms, we propose using a complex-valued least-squares (CLS) framework. Since the relationship in (9) holds for an arbitrary time instant n, by assuming that the system parameters are time-invariant within a sliding window consisting of L consecutive DFT fundamental components, we have

$$\begin{bmatrix} \hat{v}_{n-1} \\ \hat{v}_{n-2} \\ \vdots \\ \hat{v}_{n-L} \end{bmatrix} w = \begin{bmatrix} \hat{v}_n \\ \hat{v}_{n-1} \\ \vdots \\ \hat{v}_{n-L+1} \end{bmatrix} + \begin{bmatrix} \hat{v}_{n-2} \\ \hat{v}_{n-3} \\ \vdots \\ \hat{v}_{n-L-1} \end{bmatrix}. \quad (20)$$

Upon defining $\hat{\mathbf{v}}_n = [\hat{v}_n, \ldots, \hat{v}_{n-L+1}]$, this gives

$$\hat{\mathbf{v}}_{n-1} w = \hat{\mathbf{v}}_n + \hat{\mathbf{v}}_{n-2}. \quad (21)$$

We next quantify the extent to which the time-series relationship among three consecutive DFT fundamental samples in (9) breaks down in the presence of artifacts. The corresponding error vector has the form

$$\mathbf{e}_n = \hat{\mathbf{v}}_{n-1} w - (\hat{\mathbf{v}}_n + \hat{\mathbf{v}}_{n-2}). \quad (22)$$

Its Hermitian transpose is given by (since w is real)

$$\begin{aligned} \mathbf{e}_n^H &= \hat{\mathbf{v}}_{n-1}^H w^* - (\hat{\mathbf{v}}_n^H + \hat{\mathbf{v}}_{n-2}^H) \\ &= \hat{\mathbf{v}}_{n-1}^H w - (\hat{\mathbf{v}}_n^H + \hat{\mathbf{v}}_{n-2}^H) \end{aligned} \quad (23)$$

which makes it possible for the optimal coefficient w to be solved by CLS, with the additional constraint that $\hat{w}$ is real-valued. The CLS framework aims to find an optimal w in order to minimize the total mean-square error

$$\begin{aligned} J(w) &= \mathbf{e}_n^H \mathbf{e}_n \\ &= \|\hat{\mathbf{v}}_{n-1}\|^2 w^2 - 2\Re\left(\hat{\mathbf{v}}_{n-1}^H(\hat{\mathbf{v}}_n + \hat{\mathbf{v}}_{n-2})\right) w \\ &\quad + \|\hat{\mathbf{v}}_n + \hat{\mathbf{v}}_{n-2}\|^2 \end{aligned} \quad (24)$$

over a number of available observations, where $\|\cdot\|$ denotes the vector norm. To this end, the partial derivative $\partial J(w)/\partial w$ becomes

$$\frac{\partial J(w)}{\partial w} = 2\|\hat{\mathbf{v}}_{n-1}\|^2 w - 2\Re\left(\hat{\mathbf{v}}_{n-1}^H(\hat{\mathbf{v}}_n + \hat{\mathbf{v}}_{n-2})\right). \quad (25)$$

Upon setting $\partial J(w)/\partial w = 0$, the LS solution to w by the proposed CLS enhanced SDFT (CLS-SDFT) algorithm is obtained as

$$w = \frac{\Re\left(\hat{\mathbf{v}}_{n-1}^H(\hat{\mathbf{v}}_n + \hat{\mathbf{v}}_{n-2})\right)}{\|\hat{\mathbf{v}}_{n-1}\|^2}. \quad (26)$$

Observe that the real-valued property of w has now been guaranteed and, hence, the system frequency $\hat{f}$ estimated by the CLS-SDFT algorithm is given by

$$\hat{f} = f_\circ + \Delta f = \frac{f_s}{2\pi} \cos^{-1}\left(\frac{w}{2}\right). \quad (27)$$

In the next stage, we consider how to establish the CLS framework on the basis of the SDFT$_m$ algorithm, specifically de-

signed for frequency estimation of harmonic-polluted system voltages. To this end, upon revisiting (18), the estimation error vector $\mathbf{e}_n$ can be expressed as

$$\mathbf{e}_n = w\hat{\mathbf{p}}_{n-1} - (\hat{\mathbf{p}}_n + \hat{\mathbf{p}}_{n-2}) \tag{28}$$

where $\hat{\mathbf{p}}_n = [\hat{p}_n, \hat{p}_{n-1}, \ldots, \hat{p}_{n-L+1}]^T$. From (17), the estimation error vector $\mathbf{e}_n$ can be further evaluated as

$$\begin{aligned}\mathbf{e}_n = wf(w)\hat{\mathbf{v}}_{n-2} - (w + f(w))(\hat{\mathbf{v}}_{n-3} + \hat{\mathbf{v}}_{n-1}) \\ +\hat{\mathbf{v}}_{n-4} + 2\hat{\mathbf{v}}_{n-2} + \hat{\mathbf{v}}_n\end{aligned} \tag{29}$$

while its Hermitian transpose is

$$\begin{aligned}\mathbf{e}_n^H = wf(w)\hat{\mathbf{v}}_{n-2}^H - (w + f(w))(\hat{\mathbf{v}}_{n-3} + \hat{\mathbf{v}}_{n-1})^H \\ +(\hat{\mathbf{v}}_{n-4} + 2\hat{\mathbf{v}}_{n-2} + \hat{\mathbf{v}}_n)^H.\end{aligned} \tag{30}$$

This also guarantees the real-valued nature of w and $f(w)$. After some algebraic manipulations, the total mean-square error $J(w)$ becomes

$$\begin{aligned}J(w) &= \mathbf{e}_n^H \mathbf{e}_n \\ &= \|\hat{\mathbf{v}}_{n-2}\|^2 w^2 f^2(w) + \|\hat{\mathbf{v}}_{n-3} + \hat{\mathbf{v}}_{n-1}\|^2 (w + f(w))^2 \\ &\quad + \|\hat{\mathbf{v}}_{n-4} + 2\hat{\mathbf{v}}_{n-2} + \hat{\mathbf{v}}_n\|^2 - 2\Re((\hat{\mathbf{v}}_{n-3} + \hat{\mathbf{v}}_{n-1})^H \hat{\mathbf{v}}_{n-2}) \\ &\quad \cdot wf(w)(w + f(w)) + 2\Re((\hat{\mathbf{v}}_{n-4} + 2\hat{\mathbf{v}}_{n-2} + \hat{\mathbf{v}}_n)^H \hat{\mathbf{v}}_{n-2}) \\ &\quad \cdot wf(w) - 2\Re((\hat{\mathbf{v}}_{n-4} + 2\hat{\mathbf{v}}_{n-2} + \hat{\mathbf{v}}_n)^H (\hat{\mathbf{v}}_{n-3} + \hat{\mathbf{v}}_{n-1})) \\ &\quad \cdot (w + f(w)).\end{aligned} \tag{31}$$

By setting the partial derivative $\partial J(w)/\partial w = 0$, we arrive at the polynomial equation for the optimal coefficient w obtained by the proposed CLS enhanced SDFT_m($\mathrm{CLS\text{-}SDFT}_m$) algorithm, in the form

$$\begin{aligned}&\|\hat{\mathbf{v}}_{n-2}\|^2 (wf^2(w) + w^2 f(w)f'(w)) + \|\hat{\mathbf{v}}_{n-3} + \hat{\mathbf{v}}_{n-1}\|^2 \\ &\cdot (w + f(w))(1 + f'(w)) - \Re((\hat{\mathbf{v}}_{n-3} + \hat{\mathbf{v}}_{n-1})^H \mathbf{v}_{n-2}) \\ &\cdot (2wf(w) + f'(w)w^2 + f^2(w) + 2wf(w)f'(w)) \\ &- \Re((\hat{\mathbf{v}}_{n-4} + 2\hat{\mathbf{v}}_{n-2} + \hat{\mathbf{v}}_n)^H (\hat{\mathbf{v}}_{n-3} + \hat{\mathbf{v}}_{n-1}))(1 + f'(w)) \\ &+ \Re((\hat{\mathbf{v}}_{n-4} + 2\hat{\mathbf{v}}_{n-2} + \hat{\mathbf{v}}_n)^H \hat{\mathbf{v}}_{n-2})(f(w) + wf'(w)) = 0\end{aligned} \tag{32}$$

where $f'(w) = \partial f(w)/\partial w$. Note that like within the original SDFT_m algorithm, this polynomial equation contains multiple roots for w, however, the correct value of w can be selected by employing the reasonable assumption that the system frequency does not deviate from the nominal frequency f_o too much; therefore, the value of w is close to $2\cos(2\pi/N)$. Note that (32) is valid for any integer higher order harmonic, that pollutes power system voltages. Here, for illustration purposes, we provide the detailed expression of (32) for $m = 3$; in the same spirit, expressions can be obtained when other higher order harmonics are involved. For $m = 3$, we have

$$\begin{aligned}f(w) &= w^3 - 3w \\ f'(w) &= 3w^2 - 3 \\ f^2(w) &= w^6 - 6w^4 + 9w^2.\end{aligned} \tag{33}$$

Substituting (33) into (32), we finally arrive at the polynomial function of w by the proposed $\mathrm{CLS\text{-}SDFT}_3$ algorithm, given in (34) at the bottom of the page.

III. Simulations

To verify the performance advantages of the proposed complex-valued least squares enhanced SDFT (CLS-SDFT) algorithms over the original ones, numerical simulations on various types of voltage signals encountered in the real power system were conducted in the MATLAB programming environment. This includes noise and harmonic contaminations, frequency drift, power oscillations, and sudden power changes. A comparison of the results with a newly developed LS-based technique [8] is also presented to demonstrate the merit of the proposed method. In the implementation of all the considered algorithms, the nominal system frequency f_o and the sampling frequency f_s of the simulated power systems were fixed at $f_o = 50$ Hz and $f_s = 1600$ Hz, respectively; therefore, $N = f_s/f_o = 32$ samples of the system voltage were required to calculate the DFT fundamental component, while for a fair performance comparison, the observation length of the LS method was also set to $N = 32$. As required for practical implementations, a third-order low-pass infinite impulse response (IIR) Butterworth filter with a crossover frequency at 20 Hz was employed to postfilter the frequency estimates, when handling the voltages in the presence of noise or harmonics [33]. The observation length of the proposed SDFT algorithms was fixed at $L = 5$.

We first performed the statistical variance and bias analysis of all considered frequency estimators for a noisy power system. The system frequency $f = f_o + \triangle f$ was 50.5 Hz, and deviated from the nominal 50 Hz, resulting in an asynchronous sampling situation. The pure sinusoidal voltage was contaminated with zero-mean Gaussian noise, giving $v(k) = \cos(2\pi f k \triangle \mathrm{T} + 0.1\pi) + n(k)$, to which the white noise was added with various SNRs. Fig. 1(a) and (b), respectively, illustrates the estimation variance and the estimation bias of all the considered frequency estimators against different levels of noise. The consistent performance advantages of the SDFT-based algorithms over the LS algorithm can be observed and, as designed, the proposed CLS-SDFT algorithm using an observation window with multiple samples exhibited better noise rejection than the original

$$\begin{aligned}&4\|\hat{\mathbf{v}}_{n-2}\|^2 w^7 - 7\Re\left(\hat{\mathbf{v}}_{n-2}^H(\hat{\mathbf{v}}_{n-3} + \hat{\mathbf{v}}_{n-1})\right) w^6 + 3(\|\hat{\mathbf{v}}_{n-3} + \hat{\mathbf{v}}_{n-1}\|^2 - 6\|\hat{\mathbf{v}}_{n-2}\|^2)w^5 + 25\Re(\hat{\mathbf{v}}_{n-2}^H(\hat{\mathbf{v}}_{n-3} + \hat{\mathbf{v}}_{n-1}))w^4 + 2(9\|\hat{\mathbf{v}}_{n-2}\|^2 \\ &- 4\|\hat{\mathbf{v}}_{n-3} + \hat{\mathbf{v}}_{n-1}\|^2 + 2\Re(\hat{\mathbf{v}}_{n-2}^H(\hat{\mathbf{v}}_{n-4} + 2\hat{\mathbf{v}}_{n-2} + \hat{\mathbf{v}}_n)))w^3 - 3(\Re((\hat{\mathbf{v}}_{n-3} + \hat{\mathbf{v}}_{n-1})^H(\hat{\mathbf{v}}_{n-4} + 2\hat{\mathbf{v}}_{n-2} + \hat{\mathbf{v}}_n)) + 6\Re\hat{\mathbf{v}}_{n-2}^H(\hat{\mathbf{v}}_{n-3} + \hat{\mathbf{v}}_{n-1})))w^2 \\ &+ 2(2\|\hat{\mathbf{v}}_{n-2}\|^2 - 6\Re(\hat{\mathbf{v}}_{n-2}^H(\hat{\mathbf{v}}_{n-4} + 2\hat{\mathbf{v}}_{n-2} + \hat{\mathbf{v}}_n)))w + 2\Re((\hat{\mathbf{v}}_{n-3} + \hat{\mathbf{v}}_{n-1})^H(\hat{\mathbf{v}}_{n-4} + 2\hat{\mathbf{v}}_{n-2} + \hat{\mathbf{v}}_n)) = 0.\end{aligned} \tag{34}$$

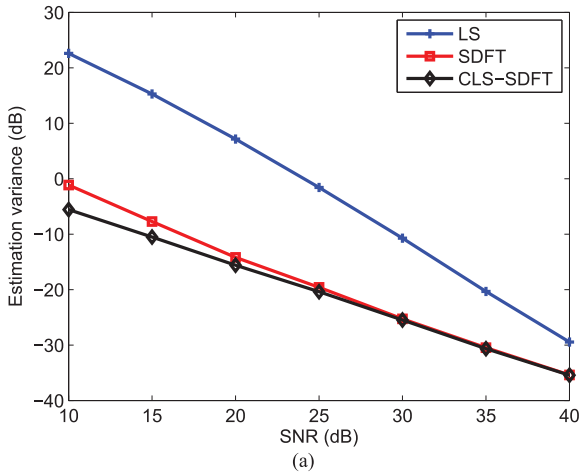

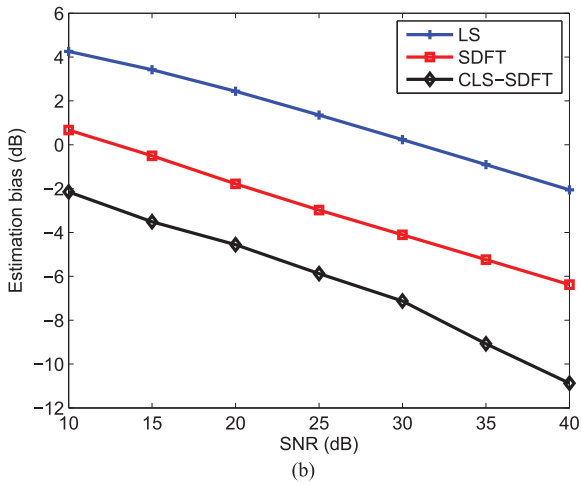

Fig. 1. Performance comparison among all of the considered frequency estimation algorithms for a noisy power system and against different SNRs. (a) Estimation variance. (b) Estimation bias. The frequency estimates have been postfiltered by a low-pass IIR filter.

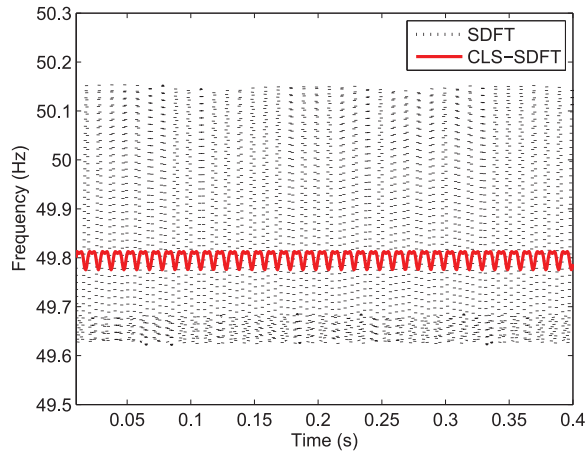

Fig. 2. Performance comparison between the proposed CLS-SDFT and the original SDFT frequency estimation algorithms for a moderately harmonically distorted power system, where $v(k) = \cos(2\pi fk\triangle \mathrm{T} + 0.3\pi) + 0.2\cos(6\pi fk\triangle \mathrm{T} - 0.1\pi)$, and $f = f_{\mathrm{o}} + \triangle f = 49.8$ Hz.

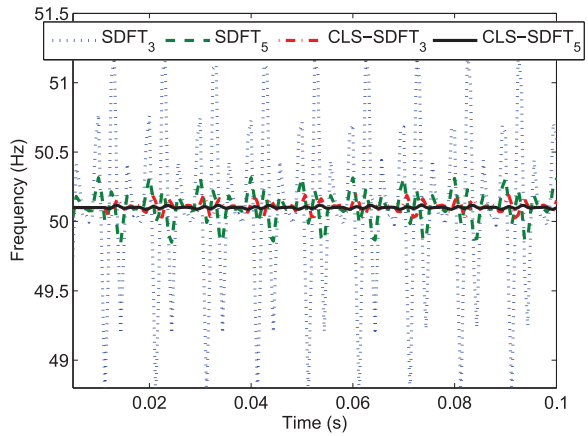

Fig. 3. Performance comparison between the proposed CLS-SDFT and the original SDFT frequency estimation algorithms (without postfiltering) for a heavily harmonically distorted power system, where $v(k) = \cos(2\pi fk\triangle \mathrm{T} - 0.1\pi) + 0.2\cos(6\pi fk\triangle \mathrm{T} + 0.3\pi) + 0.1\cos(10\pi fk\triangle \mathrm{T} + 0.2\pi) + 0.05\cos(14\pi fk\triangle \mathrm{T} + 0.1\pi)$, and $f = f_{\mathrm{o}} + \triangle f = 50.1$ Hz.

one. The results were obtained by averaging 1000 independent trials.

In the next set of simulations, we considered a moderately harmonically distorted power system, where the system frequency f was deviated to 49.8 Hz and the voltages $v(k) = \cos(2\pi fk\triangle \mathrm{T} + 0.3\pi) + 0.2\cos(6\pi fk\triangle \mathrm{T} - 0.1\pi)$. The performances of the original SDFT and the proposed CLS-SDFT algorithms in such a situation are given in Fig. 2. Since the original SDFT algorithm does not consider higher order harmonics in its underlying mathematical formulation, the existence of this third harmonic within the voltage causes the breakdown of the time-series relationship among the three consecutive DFT fundamental components given in (9), which, in turn, renders frequency estimates inaccurate. On the contrary, by design, the proposed CLS-SDFT algorithm is based on the minimization of the degree of the breakdown of such a relationship, and it thus provides higher immunity to the harmonic pollution while an observation window lasting for 5 samples enables it to track the system frequency more accurately with a maximum estimation bias of 0.0129 Hz compared with 0.3545 Hz obtained by the original SDFT algorithm. By applying the low-pass filtering technique on the frequency estimates, the estimate ripples can be further suppressed; the maximum estimation bias of the original SDFT and the proposed CLS-SDFT algorithms were, respectively, reduced to 0.0019 and 0.0005 Hz.

We next considered the frequency estimation performances of the proposed CLS-SDFT$_m$ algorithm and the original SDFT$_m$ for a heavily harmonic distorted power system, where the third, fifth, and seventh harmonics were added to the voltages, giving $v(k) = \cos(2\pi fk\triangle \mathrm{T} - 0.1\pi) + 0.2\cos(6\pi fk\triangle \mathrm{T} + 0.3\pi) + 0.1\cos(10\pi fk\triangle \mathrm{T} + 0.2\pi) + 0.05\cos(14\pi fk\triangle \mathrm{T} + 0.1\pi)$, and the system frequency f was deviated from the nominal 50 Hz at 50.1 Hz. As shown in Fig. 3, SDFT$_3$ and SDFT$_5$ rendered unavoidable frequency oscillations due to the submodelling of the system voltage, for instance, the fifth and seventh harmonics were not considered in the underlying voltage modelling of the SDFT$_3$ algorithm. However, the proposed CLS framework enabled both algorithms to track the exact system frequency more accurately;

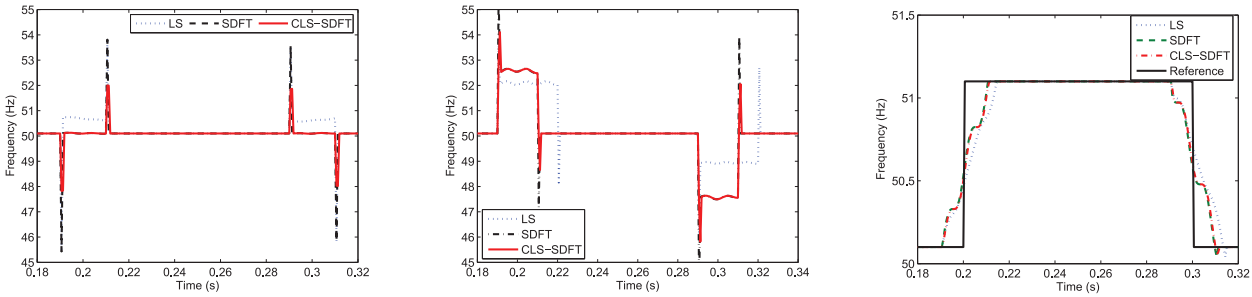

(a) (b) (c)

Fig. 4. Frequency responses of all considered algorithms under power system abrupt change. (a) Amplitude steps. (b) Phase-angle steps. (c) Frequency steps.

TABLE I
MAXIMUM ESTIMATION ERRORS OF SDFT-BASED FREQUENCY ESTIMATORS IN THE PRESENCE OF HEAVY HARMONICS AFTER APPLYING THE POSTFILTERING TECHNIQUE

	Maximum estimation error (mHz)
SDFT_3	15.7
SDFT_5	2.92
CLS-SDFT_3	7.71
CLS-SDFT_5	0.46

the maximum frequency estimation bias of CLS-SDFT_3 and CLS-SDFT_5 was, respectively, 0.0851 Hz and 0.0176 Hz. The postfiltering technique was able to suppress ripples in the estimate effectively, and the final results were provided in Table I. It is worth mentioning that the original SDFT_{357} frequency estimation algorithm is also able to deal with this paradigm, by employing matched voltage modeling, however, the advantage of the proposed CLS framework is in that by minimizing the degree of system modelling breakdown, it equips SDFT algorithms with robustness in frequency estimation even when the voltage modelling is suboptimal; for instance, in the presence of noise and unexpected higher order harmonics.

We next considered the frequency estimation performances of the LS, the original SDFT, and the proposed CLS-SDT algorithms in the cases where the power system experiences abrupt changes in the amplitude, phase angle, and system frequency. These disturbances may result from faults or switching operations, and were modeled by step changes in the corresponding parameters as specified in the IEEE standard C37.118 [34]. The simulated power systems were initialized with $f = f_\text{o} + \triangle f = 50.1$ Hz, giving $v(k) = \cos(2\pi f k \triangle \text{T} + 0.1\pi)$, and they experienced a 10% step in amplitude, a $\pi/10$ step in phase angle and a 1 Hz step in frequency at 0.2 s, respectively, and were reversed back to the initial condition at 0.3 s. As illustrated in Fig. 4, all of the considered frequency estimators suffered from transition effects during the disturbances. In all cases, the original SDFT and the proposed CLS-SDFT exhibited a similar but shorter settling period compared with the LS-based frequency estimator. It has to be pointed out that the response time of the proposed CLS-SDFT algorithm depends on the length of the voltage observations. Its response time to power system abrupt changes is expected to be prolonged when a larger number of voltage observations is involved. However, the advantages of the proposed CLS framework are in a relatively short observation window, for instance, an observation window with 5 samples used in these experiments is sufficient. This equips the SDFT algorithm with enhanced robustness in the presence of noise and harmonics-contaminated environments, as indicated by the previous simulations.

Power systems may experience modulations in amplitude, phase angle, and system frequency modulations, when the balance of power generation and consumption is violated due to system disturbances, such as a fault or loss of load. We first considered the case when the power system, whose system frequency was fixed at 49.9 Hz, experienced a slow 0.2 p.u. voltage amplitude modulation at 1 Hz. As shown in Fig. 5(a), the proposed CLS-SDFT algorithm produced the smallest estimation error (with a maximum of 2.5 mHz) among all of the considered frequency estimators. We next considered the simulated power system which experienced sinusoid phase modulation, given by

$$v(k) = \cos(2\pi f_\text{o} k \triangle \text{T} + A_\phi \cos(2\pi f_\phi k \triangle \text{T} + \phi_\phi)) \quad (35)$$

where A_ϕ was 0.2 p.u., f_ϕ was 1 Hz, and ϕ_ϕ was 0.4 π. The equivalent modulated system frequency can be expressed as

$$f(k) = f_\text{o} - A_\phi f_\phi \sin(2\pi f_\phi k \triangle \text{T} + \phi_\phi)). \quad (36)$$

Simulation results in Fig. 5(b) show that the frequency estimates by the SDFT-based algorithms tracked the modulated system frequency more quickly and accurately than the LS-based frequency estimator under this slowly changing condition. As shown in Fig. 5(c), these frequency tracking advantages can be also observed in a more dynamical frequency modulation case, where the system experienced combined sinusoid frequency variations, described by

$$f(t) = \begin{cases} f_\text{o} + 2\sin(4\pi(t-0.1)) + \\ \sin(32\pi(t-0.1)), & 0.1\text{ s} \le t < 0.75\text{ s} \\ f_\text{o}, & \text{elsewhere} \end{cases} . \quad (37)$$

The frequency-tracking capabilities of all considered frequency estimators in the context of frequency ramp variations were investigated next. Two examples of 1 and -1 Hz/s ramps were considered. The responses of all the considered frequency estimators for the positive and negative rate of change are shown in Fig. 6(a) and (b), respectively. Again, the frequency estimates by SDFT-based algorithms followed the ramps very closely, while the LS algorithm had fairly large errors as the frequency deviated from its nominal value.

In the last set of simulations, a real-world power system was considered. The phase-ground voltage was recorded at a 110/20/10 kV transformer station. The measured voltage with

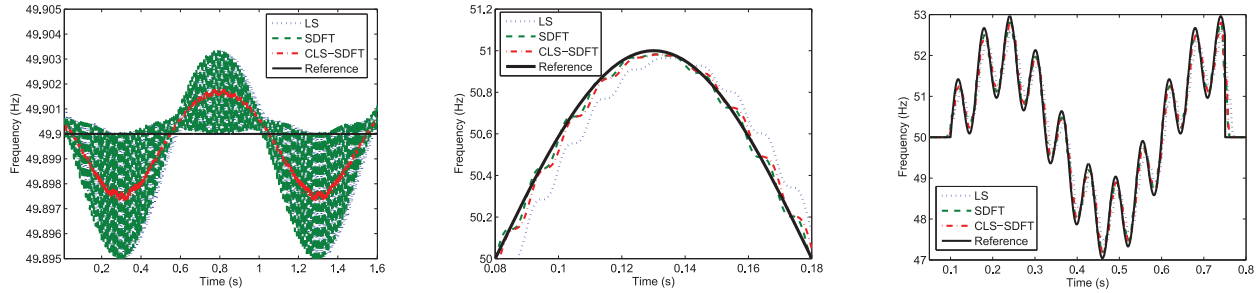

Fig. 5. Frequency responses of all the considered algorithms under power system modulations. (a) Amplitude modulation. (b) Phase modulation. (c) Frequency modulation.

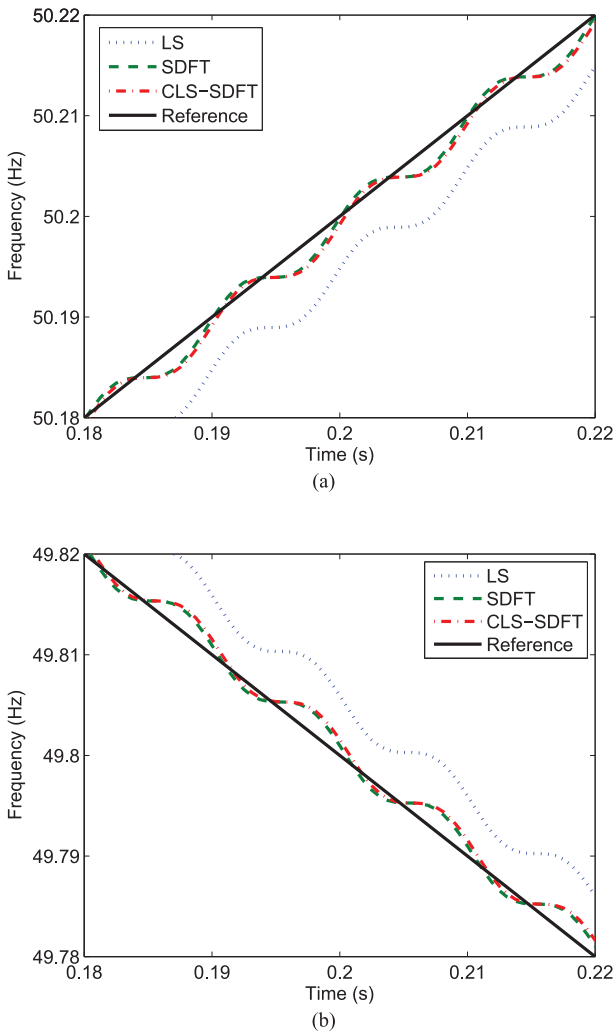

Fig. 6. Responses of all considered algorithms for frequency ramps. (a) Frequency rise at a rate of 1 Hz/s. (b) Frequency decay at a rate of 1 Hz/s.

a system frequency around 50 Hz was sampled at a rate of 1 kHz and was normalized with respect to its normal peak voltage value. The frequency tracking performances of all the algorithms considered for this experiment are given in Fig. 7. To meet the commercial needs, the frequency estimates by all approaches at time instant k were postfiltered using the filter given by $f(k) = 1/8\hat{f}(k) + 7/8\hat{f}_{\text{mean}}(k)$, where $\hat{f}_{\text{mean}}(k)$ was measured for every cycle. Conforming with the analysis

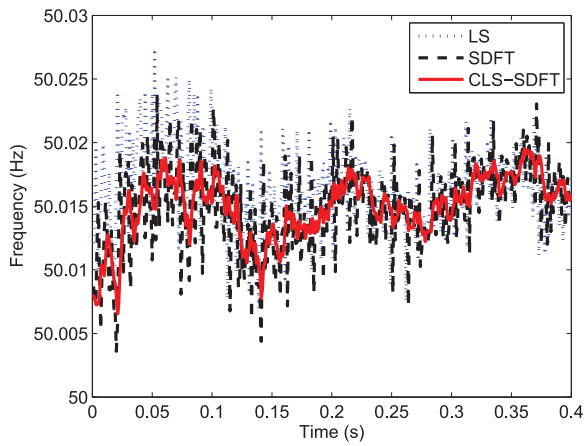

Fig. 7. Frequency estimation by the least squares (LS), the original SDFT, and the proposed CLS-SDFT algorithms for real-world system voltages.

TABLE II
ESTIMATION VARIANCES OF ALL CONSIDERED ALGORITHMS FOR THE REAL-WORLD SYSTEM VOLTAGES

LS	SDFT	CLS-SDFT
1.2106e-005	1.0922e-005	6.1904e-006

in Section II, the proposed CLS framework clearly equips the SDFT algorithm with enhanced robustness in the presence of measurement noise, as evidenced by a smaller estimation variance, given in Table II.

IV. CONCLUSIONS

We have introduced the CLS framework in order to equip the original SDFT algorithms with robustness to noise and harmonics, key issues in practical applications. This has been achieved by employing the error vector to represent the breakdown of the relationship between the consecutive DFT fundamental components within a sliding window under consideration. The so-introduced mean-square minimization allows the SDFT algorithms to provide robust frequency estimates even when the underlying voltage model is suboptimal, such as in the presence of measurement noises or unexpected higher order harmonics. The performance advantage of the proposed CLS framework has been verified by simulations over various power system conditions, as well as for a real-world measurement.

REFERENCES

[1] J. Z. Yang and C. W. Liu, "A precise calculation of power system frequency and phasor," *IEEE Trans. Power Del.*, vol. 15, no. 2, pp. 494–499, Apr. 2000.

[2] J. Z. Yang and C. W. Liu, "A precise calculation of power system frequency," *IEEE Trans. Power Del.*, vol. 16, no. 3, pp. 361–366, Jun. 2001.

[3] M. M. Begovic, P. M. Djuric, S. Dunlap, and A. G. Phadke, "Frequency tracking in power networks in the presence of harmonics," *IEEE Trans. Power Del.*, vol. 8, no. 2, pp. 480–486, Apr. 1993.

[4] H. Karimi, M. Karimi-Ghartemani, and M. R. Iravani, "Estimation of frequency and its rate of change for applications in power systems," *IEEE Trans. Power Del.*, vol. 19, no. 2, pp. 472–480, Apr. 2004.

[5] M. Karimi-Ghartemani, B.-T. Ooi, and A. Bakhshai, "Application of enhanced phase-locked loop system to the computation of synchrophasors," *IEEE Trans. Power Del.*, vol. 26, no. 1, pp. 22–32, Feb. 2011.

[6] M. Mojiri, M. Karimi-Ghartemani, and A. Bakhshai, "Estimation of power system frequency using an adaptive notch filter," *IEEE Trans. Instrum. Meas.*, vol. 56, no. 6, pp. 2470–2477, Dec. 2007.

[7] M. S. Sachdev and M. M. Giray, "A least error squares technique for determining power system frequency," *IEEE Trans. Power App. Syst.*, vol. PAS-104, no. 2, pp. 437–444, Feb. 1985.

[8] A. Abdollahi and F. Matinfar, "Frequency estimation: A least-squares new approach," *IEEE Trans. Power Del.*, vol. 26, no. 2, pp. 790–798, Apr. 2011.

[9] A. K. Pradhan, A. Routray, and A. Basak, "Power system frequency estimation using least mean square technique," *IEEE Trans. Power Del.*, vol. 20, no. 3, pp. 761–766, Jul. 2005.

[10] Y. Xia and D. P. Mandic, "Widely linear adaptive frequency estimation of unbalanced three-phase power systems," *IEEE Trans. Instrum. Meas.*, vol. 61, no. 1, pp. 74–83, Jan. 2012.

[11] Y. Xia, S. C. Douglas, and D. P. Mandic, "Adaptive frequency estimation in smart grid applications: Exploiting noncircularity and widely linear adaptive estimators," *IEEE Signal Process. Mag.*, vol. 29, no. 5, pp. 44–54, Sep. 2012.

[12] P. K. Dash, A. K. Pradhan, and G. Panda, "Frequency estimation of distorted power system signals using extended complex Kalman filter," *IEEE Trans. Power Del.*, vol. 14, no. 3, pp. 761–766, Jul. 1999.

[13] A. Routray, A. K. Pradhan, and K. P. Rao, "A novel Kalman filter for frequency estimation of distorted signals in power systems," *IEEE Trans. Instrum. Meas.*, vol. 51, no. 3, pp. 469–479, Jun. 2002.

[14] Z. Salcic, N. S. Kiong, and Y. Wu, "An improved Taylor method for frequency measurement in power systems," *IEEE Trans. Instrum. Meas.*, vol. 58, no. 9, pp. 3288–3294, Sep. 2009.

[15] J. Ren and M. Kezunovic, "A hybrid method for power system frequency estimation," *IEEE Trans. Power Del.*, vol. 27, no. 3, pp. 1252–1259, Jul. 2012.

[16] V. V. Terzija, M. B. Djuric, and B. D. Kovacevic, "Voltage phasor and local system frequency estimation using Newton type algorithm," *IEEE Trans. Power Del.*, vol. 9, no. 3, pp. 1368–1374, Jul. 1994.

[17] H.-J. Jeon and T.-G. Chang, "Iterative frequency estimation based on MVDR spectrum," *IEEE Trans. Power Del.*, vol. 25, no. 2, pp. 621–630, Apr. 2010.

[18] P. K. Dash and S. Hasan, "A fast recursive algorithm for the estimation of frequency, amplitude, and phase of noisy sinusoid," *IEEE Trans. Ind. Electron.*, vol. 58, no. 10, pp. 4847–4856, Oct. 2011.

[19] F. Zhang, Z. Geng, and W. Yuan, "The algorithm of interpolating windowed FFT for harmonic analysis of electric power system," *IEEE Trans. Power Del.*, vol. 16, no. 2, pp. 160–164, Apr. 2001.

[20] H. Qian, R. Zhao, and T. Chen, "Interharmonics analysis based on interpolating windowed FFT algorithm," *IEEE Trans. Power Del.*, vol. 22, no. 2, pp. 1064–1069, Apr. 2007.

[21] S. Schuster, S. Scheiblhofer, and A. Stelzer, "The influence of windowing on bias and variance of DFT-based frequency and phase estimation," *IEEE Trans. Instrum. Meas.*, vol. 58, no. 6, pp. 1975–1990, Jun. 2009.

[22] T. Radil, P. M. Ramos, and A. C. Serra, "New spectrum leakage correction algorithm for frequency estimation of power system signals," *IEEE Trans. Instrum. Meas.*, vol. 58, no. 5, pp. 1670–1679, May 2009.

[23] C. Candan, "A method for fine resolution frequency estimation from three DFT samples," *IEEE Signal Process. Lett.*, vol. 18, no. 6, pp. 351–354, Jun. 2011.

[24] D. Petri, D. Fontanelli, and D. Macci, "A frequency-domain algorithm for dynamic synchrophasor and frequency estimation," *IEEE Trans. Instrum. Meas.*, vol. 63, no. 10, pp. 2330–2340, Oct. 2014.

[25] D. Belega, D. Macii, and D. Petri, "Fast synchrophasor estimation by means of frequency-domain and time-domain algorithms," *IEEE Trans. Instrum. Meas*, vol. 63, no. 2, pp. 388–401, Feb. 2014.

[26] H. Wen, S. Guo, Z. Teng, F. Li, and Y. Yang, "Frequency estimation of distorted and noisy signals in power systems by FFT-based approach," *IEEE Trans. Power Syst.*, vol. 29, no. 2, pp. 765–774, Mar. 2014.

[27] M. Wang and Y. Sun, "A practical, precise method for frequency tracking and phasor estimation," *IEEE Trans. Power Del.*, vol. 19, no. 4, pp. 1547–1552, Oct. 2004.

[28] M. Wang and Y. Sun, "A practical method to improve phasor and power measurement accuracy of DFT algorithm," *IEEE Trans. Power Del.*, vol. 21, no. 3, pp. 1054–1062, Jul. 2006.

[29] D. Borkowski and A. Bien, "A practical, precise method for frequency tracking and phasor estimation," *IEEE Trans. Power Del.*, vol. 24, no. 3, pp. 1004–1013, Jul. 2009.

[30] J. R. de Carvalho, C. A. Duque, M. A. A. Lima, D. V. Coury, and P. F. Ribeiro, "A novel DFT-based method for spectral analysis under time-varying frequency conditions," *Elect. Power Syst. Res.*, vol. 108, pp. 74–81, 2014.

[31] J. K. Hwang and P. N. Markham, "Power system frequency estimation by reduction of noise using three digital filters," *IEEE Trans. Instrum. Meas.*, vol. 63, no. 2, pp. 402–409, Feb. 2014.

[32] A. G. Phadke, J. S. Thorp, and M. G. Adamiak, "A new measurement technique for tracking voltage phasors, local system frequency, and rate of change of frequency," *IEEE Trans. Power App. Syst.*, vol. PAS-102, no. 5, pp. 1025–1038, May 1983.

[33] M. Akke, "Frequency estimation by demodulation of two complex signals," *IEEE Trans. Power Del.*, vol. 12, no. 1, pp. 157–163, Jan. 1997.

[34] *IEEE Standard for Synchrophasors for Power Systems*, IEEE Standard C37.118-2011, Dec. 2011.

Yili Xia (M'11) received the B.Eng. degree in information engineering from Southeast University, Nanjing, China, in 2006, the M.Sc. (Hons.) degree in communications and signal processing, and the Ph.D. degree in adaptive signal processing from Imperial College London, London, U.K., in 2007 and 2011, respectively.

Since 2013, he has been an Associate Professor with the School of Information and Engineering, Southeast University. His research interests include complex-valued linear and nonlinear adaptive filters, complex-valued statistical analysis, and their applications on power systems.

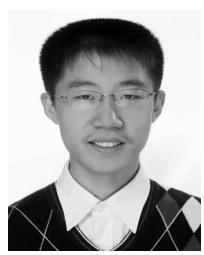

Yukun He is currently pursuing the B.Eng. degree in electronic science and technology at Southeast University, Nanjing, China.

His research interests include complex-valued statistical analysis and power system analysis.

Kai Wang received the Ph.D. degree in signal processing from the School of Information and Engineering, Southeast University, Nanjing, China, in 2009.

Currently, he is an Associate Professor of Signal Processing at Southeast University. His research interests include signal processing, chaotic cryptosystems, and complex networks.

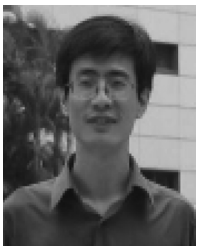

Wenjiang Pei received the M.S. and Ph.D. degrees in measurement technology and instrumentation from Nanjing University of Aeronautics and Astronautics, Nanjing, China, in 1995 and 1997, respectively.

Currently, he is a Professor in the School of Information and Engineering, Southeast University, Nanjing, China. His research interests include neural networks, nonlinear dynamics, and signal processing in networking.

Zoran Blazic received the Dipl.Eng. degree in automation and computer engineering from the Faculty of Electrical Engineering, University of Banja Luka, Bosnia and Herzegovina, in 1991.

Since 1993, he has been with the Transmission Company in Bosnia and Herzegovina, in various positions. Currently, he is Head of SCADA and Automation Department Transco BiH/OP Banja Luka. His current research interests are in the control and operation of power transmission system, wide-area measurement systems, and applications of IEC 61850 standards in modern substations.

Dr. Blazic is a member of Serbian CIGRE SC D2.

Danilo P. Mandic (M'99–SM'03–F'12) received the Ph.D. degree in nonlinear adaptive signal processing from Imperial College London, London, U.K., in 1999, where he is currently a Professor in Signal Processing.

He has been working in the area of nonlinear adaptive signal processing, multivariate data analysis, and nonlinear dynamics. He has been a Guest Professor at Katholieke Universiteit Leuven, Leuven, Belgium; the Tokyo University of Agriculture and Technology, Tokyo, Japan; and Westminster University, London, U.K.; and a Frontier Researcher at RIKEN, Tokyo, Japan. His publication record includes two research monographs entitled *Recurrent Neural Networks for Prediction*: *Learning Algorithms*, *Architectures and Stability* (Wiley, 2001) and *Complex Valued Nonlinear Adaptive Filters*: *Noncircularity*, *Widely Linear and Neural Models* (Wiley, 2009), an edited book titled *Signal Processing Techniques for Knowledge Extraction and Information Fusion* (Springer, 2008), and more than 200 publications on signal and image processing. He has been an Associate Editor for the *IEEE Signal Processing Magazine*, IEEE TRANSACTIONS ON CIRCUITS AND SYSTEMS II, IEEE TRANSACTIONS ON SIGNAL PROCESSING, and IEEE TRANSACTIONS ON NEURAL NETWORKS.

Prof. Mandic has been a member of the IEEE Technical Committee on Signal Processing Theory and Methods, and has been an Associate Editor for the *International Journal of Mathematical Modelling and Algorithms*. He has produced award-winning papers and products resulting from his collaboration with industry.